J Membrane Biol (2009) 228:51–62
DOI 10.1007/s00232-009-9158-4

Three Types of Single Voltage-Dependent Potassium Channels in the Sarcolemma of Frog Skeletal Muscle

Mario Vázquez-García · Gloria Reyes-Guerrero

Received: 28 August 2008 / Accepted: 31 January 2009 / Published online: 25 February 2009

Abstract Patch-clamp experiments in the sarcolemma of frog skeletal muscle evidenced the presence of three types of voltage-dependent single-channel K^+ currents. According to their unitary conductance at a membrane voltage of +40 mV, we classified them as 16-, 13-, and 7-pS K^+ channels. The 16-pS K^+ channels are active close to a membrane voltage of −80 mV and they do not become inactivated during voltage pulses of 100 ms. Within 10 min after beginning the recording, these channels developed rundown with an exponential time course. The 13-pS K^+ channels are active near −60 mV; upon a 100-ms depolarization, they exhibited inactivation with an approximate exponential time course. The 7-pS K^+ channels were recorded at voltages positive to 0 mV. In patches containing all three types of K^+ channels, the ensemble average currents resemble the kinetic properties of the macroscopic delayed rectifier K^+ currents recorded in skeletal muscle and other tissues. In conclusion, the biophysical properties of unitary K^+ currents suggest that these single-channel K^+ currents may underlie the macroscopic delayed K^+ currents in frog skeletal muscle fibers. In addition, since the 16- and 13-pS channels were more frequently recorded, both are the main contributors to the delayed K^+ currents.

Keywords Potassium channels · Delayed rectifier · Skeletal muscle · Rundown

M. Vázquez-García (✉) · G. Reyes-Guerrero
Departamento de Fisiología, Facultad de Medicina, Universidad Nacional Autónoma de México, Apartado Postal 70250, 04510 Mexico, D.F., Mexico
e-mail: mvazquez@liceaga.facmed.unam.mx

Recent single-channel studies and molecular cloning have demonstrated the coexistence of several functionally different types of voltage-activated K^+ channels in a variety of tissues, including axons, skeletal muscle, and neurons (Hoshi and Aldrich 1988; Llano et al. 1988; Zagotta et al. 1988; Jonas et al. 1989; Martínez-Padrón and Ferrús 1997; Chen and Johnston 2004). Based on single-channel recording, it has been postulated that the macroscopic delayed rectifier K^+ current in squid giant axon represents the contribution from at least two distinct channel types (Llano et al. 1988). In addition, at least three different K^+ channels contribute to the whole-cell K^+ currents in *Drosophila* peptidergic synaptic buttons (Martínez-Padrón and Ferrús 1997). These current types are distinguishable at a single-channel level based on the voltage range of activation, inactivation properties, conductance, and other criteria. On the other hand, in voltage-clamped skeletal muscle fibers, the macroscopic delayed rectifier K^+ currents are also assumed to contain more than one type of K^+ channels (Adrian et al. 1970; Duval and Léoty 1980). Nevertheless, less is known about how many channels contribute to the macroscopic delayed rectifier currents.

For a deeper insight into potassium conductance through delayed-rectifier channels in more than one type of channel, we used the patch-clamp technique, which allows for a detailed analysis of single-channel currents (Hamill et al. 1981). Therefore, the aim of present study was to characterize some of the single-channel properties of the three voltage-activated outward K^+ channels in the sarcolemma of frog skeletal muscle. Single-channel analyses reveal that activation, as well as inactivation, of the channels can be described in terms of Hodgkin-Huxley (1952) kinetics. These findings led to the proposal that such channels are involved in the delayed rectifier K^+ currents from skeletal muscle. However, the biological significance of these

different types of channels in the total macroscopic current remains to be ascertained.

Materials and Methods

The production of spherical vesicles from the sarcolemma of frog (*Rana montezumae*) semitendinosus muscles and the electrophysiological method used in this study were as described previously (Hamill et al. 1981; Standen et al. 1984; Vázquez 1998). Briefly, we used the patch-clamp method in the inside-out configuration, following the design of Hamill et al. (1981). Patch pipettes were made on a two-stage puller (Narishige model PP-83; Tokyo) from hard glass capillaries (KIMAX-51; Kimble Glass, Toledo, OH, USA), and after they were filled with a pipette solution their resistance was 5–10 MΩ. Electrodes were coated to near their tips with Sylgard resin (Down Corning, Midland, MI, USA) and then fire-polished. In general, sealing resistances between the pipette tip and the membrane of the vesicle were ≥20 GΩ and remained stable for up to 1 h. Single-channel currents were recorded using a DAGAN patch-clamp amplifier (model 8900; Minneapolis, MN, USA). A steady potential was applied to the inside of the pipette to set the holding potential. Membrane potentials are expressed as the inside potential relative to the outside surface of the membrane, and outward currents are considered positive.

Solutions

In all experiments, the bath solution contained (mM) 120 KCl, 2 $MgCl_2$, 2 ethyleneglycoltetraacetic acid (EGTA), and 2 Na_2ATP; 4-aminopyridine (4-AP; 5 mM) was required to block A-type K^+ channels. The pipette solution consisted of (mM) 117.5 NaCl, 2.5 KCl, and 2 $CaCl_2$; tetrodotoxin (TTX, 6 μM) was required to block Na^+ currents. The bath and pipette solutions were buffered with 4-(2-hydroxyethyl)-1-piperazineethanesulphonic acid (5 mM HEPES), pH 7.2. Experiments were performed at room temperature (20–24°C).

Data Collection and Analysis

A personal computer-controlled data acquisition and pulsing. Currents were amplified to 0.1–0.2 V pA^{-1}, filtered at 2 kHz (low-pass, eight-pole Bessel filter), before being digitized at 10 kHz (Lab Master; Axon Instruments, Inverurie UK). Data were obtained in sets of voltage steps of 100-ms duration delivered at regular intervals of 1 s. Uncorrected linear capacitive and leakage currents were analogic and digitally subtracted; for digital subtraction, average blank records were appropriately scaled for the rest. Because of the presence of several single-channel current levels in the recording, the maximum likelihood method was used to estimate the number of channels (N) in the patch, i.e., those that correspond to the number of single-channel current level (Patlak and Horn 1982). The 50% threshold detection method was used to detect open and closed levels (Colquhoun and Sigworth 1995). Currents were collected and analyzed with pCLAMP software (Axon Instruments). Groups of data were compared using paired t-test or one-way ANOVA followed by Student-Newman-Keuls (SNK) post hoc test (SigmaStat; Jandel Corp.). A p-value < 0.05 was considered statistically significant. Data are expressed as mean ± standard error of the mean (SEM).

Results

We characterized three distinct types of voltage-activated K^+ channels from the skeletal muscle membrane of the frog. The ionic conditions used in our experiments were designed to isolate membrane currents through K^+ channels. Under this condition, the equilibrium potential for K^+ is −87 mV (Standen et al. 1984, 1985); the extrapolated reversal potential for all three types of K^+ currents was more negative than −80 mV. In addition, when the equilibrium potential for K^+ was 0 mV, the reversal potential changed, as expected for a K^+-selective channel, and was not different when the equilibrium potential for Cl^- was changed. Notwithstanding, we analyzed patch recordings with Cl^- solution for all experiments reported here. On the other hand, Ca-activated K^+ channels were closed owing to the virtual absence of Ca^{2+} (Barrett et al. 1982; Marty 1989), since the bath solution was nominally a Ca^{2+}-free solution. Besides, the ATP-sensitive K^+ channels were kept closed by the presence of ATP in the bath solution (Spruce et al. 1987).

Due to the nonlinear behavior of the current-voltage (I-V) relationship, the single-channel conductance is expressed as the chord conductance (γ). The designation of the three voltage-activated K^+ channels is based on their γ at a voltage membrane of +40 mV, i.e., the 16-pS K^+ channel, 13-pS K^+ channel, and 7-pS K^+ channel. The mean of single-channel conductances of the three K^+ channels was statistically different ($p < 0.05$) according to all pairwise comparisons by the parametric one-way ANOVA test followed the SNK post hoc test.

The 16-pS K^+ Channel

Single-channel recordings showed a 16-pS K^+ channel. This channel is activated at voltages greater than or equal to −80 mV. The membrane potential was depolarized from

a holding potential of −100 mV to +40 mV, in steps of 20 mV, for a period of 100 ms. The 16-pS K^+ channel invariably developed rundown, therefore all analyses were performed before the channel reached rundown. Figure 1 shows records of this type of single-channel K^+ currents during voltage steps ranging from −40 to +40 mV. In response to depolarizing pulses, the channel exhibited openings that varied in a stepwise manner with time and brief latency and typically displayed openings with long open times during almost the whole depolarization time (Fig. 1a). Activity of the 16-pS K^+ channel was measured in isolation from the other two channels in 59 patches from a total of 150 patches. The single-channel current levels at a given membrane potential were obtained from the amplitude histograms of all data points from 100 records similar to those shown in Fig. 1a. The current amplitude histograms for +40-mV voltage steps fitted well the sum of two Gaussian distributions (Fig. 1b). The current amplitude estimated from the fit was 2.54 pA. The single-channel current taken from the fit of the amplitude histograms was plotted as a function of voltage (Fig. 1c). The mean of single-channel currents ($n = 10$) showed a nonlinear current-voltage relationship according to the recognized feature of the delayed rectifier K^+ channel (Adrian et al. 1970; Conti and Neher 1980; Rudy 1988; Standen et al. 1985). In addition, just as the delayed rectifier currents, our records were characterized by the absence of detectable channel activity at negative potentials near the resting potential; therefore, the reversal potential was not obtained directly. The extrapolated reversal potential of the current is −90 ± 2.3 mV ($n = 10$), whereas, taking the value for P_{Na}:$P_K = 0.01$ (Standen et al. 1984, 1985), the equilibrium potential of K^+ is −87 mV. Under this ionic condition for K^+, γ is 26.1 ± 2, 20.3 ± 1, and 16 ± 0.8 pS ($n = 10$) at −40, 0, and +40 mV, respectively. In order to verify the ionic selectivity of the channel, the unitary currents were also recorded in symmetrical solutions of K^+ (120 mM). This produced a shift in the current-voltage relationship to the right (data not shown), with a reversal potential near to 0 mV ($n = 8$), as would be expected for a channel predominantly selective to K^+. The single-channel activity showed no inactivation during 100-ms depolarizing pulses ranging from −80 to +40 mV (Fig. 1a). Channel openings with short delay and the absence of inactivation during voltage steps are reflected in the ensemble average currents (Fig. 1d, e). The single-channel behavior produces an

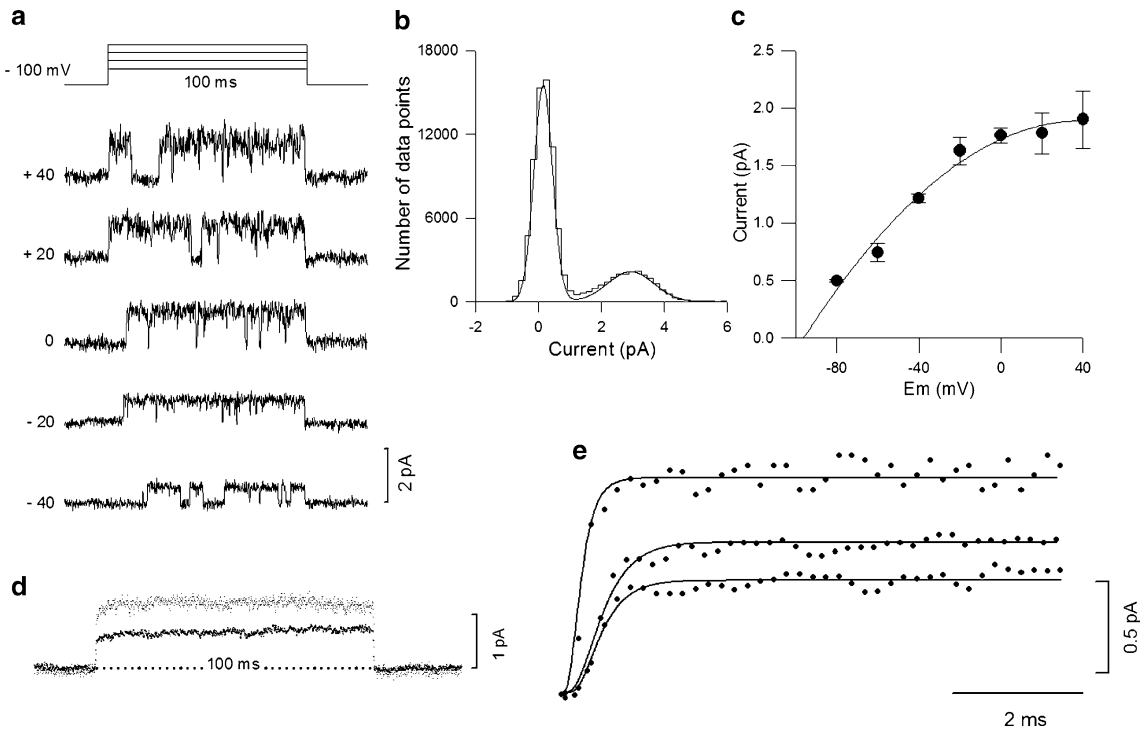

Fig. 1 Kinetic properties of 16-pS K^+ single-channel currents. **a** Voltage protocol indicated above. Currents were elicited every 1 s by voltage steps from a holding potential of −100 mV. The voltage steps indicate the closed state. **b** Amplitude histogram of all data points is shown for a +40-mV step in a. The smooth line is the sum of two Gaussian fits. **c** Mean single-channel current amplitude plotted against voltage step ($n = 10$); the curve was drawn visually through the experimental points. **d** Single-channel ensemble average currents for +40 mV (upper trace) and −40 mV (lower trace), averaged from 100 single sweeps. **e** First 8 ms of ensemble average currents for +40 mV (upper trace), 0 mV (middle trace), and −40 mV (lower trace). The smooth line represents n^4 time-course activation, where n^4 activation was calculated according to Eq. 1. Same experiment throughout **a**–**e**

ensemble average current that activates very rapidly and is a truly sustained current. Average current stays in these current levels during all the depolarization time (Fig. 1d). These characteristics are consistent with the delayed rectifier K^+ channel current data (Conti and Neher 1980; Hoshi and Aldrich 1988; Llano et al. 1988; Martínez-Padrón and Ferrús 1997).

One of the main distinctive features of the delayed rectifier K^+ currents is that their time course can be described according to Hodgkin-Huxley theoretical equations (Hodgkin and Huxley 1952; Rudy 1988). Figure 1d shows the ensemble average currents from 100 individual sweeps, from a holding potential of −100 mV to +40 mV (upper trace) and to −40 mV (bottom trace). The points in Fig. 1e show the first 8 ms of the ensemble average currents from experiments depicted in Fig. 1a; the smooth line was calculated by an equation similar to that used by Hodgkin and Huxley (1952), which approximates to

$$I_{(t)} = I_{\max}\left[1 - \exp\left(-t/\tau_a\right)\right]^n, \quad (1)$$

with $n = 4$, where $I(t)$ is the amplitude of the current at time t, I_{max} is the maximal amplitude of the current, τ_a is the time constant of the activation process. In this example, τ_a is 1.062, 0.760, and 0.078 ms at −40, 0, and +40 mV, respectively. The results show that ensemble average currents are well fitted to n^4 kinetics.

Upon excision, spontaneous rundown of channel activity was observed at approximately 8 ± 0.471 min ($n = 10$) after the recordings had begun. The rundown was time-dependent and relatively fast, so that almost-complete closure of the channels occurred with a time constant of 5.7 min (Fig. 2a). Throughout the rundown, the overall initial channel activity on patch excision was decreased dramatically, which is reflected in a diminution in the open probability to almost-zero unitary activity. As expected, the unitary current amplitude did not change during the rundown process. On the other hand, to distinguish between the rundown process and the slow inactivation (see below), voltage pulses were applied every 6 s. The time course of rundown was similar when the intervals between pulses were either 1 or 6 s (data not shown).

There is evidence that many ion channels show current rundown, and this loss of activity can be prevented or reversed by adding MgATP and/or protein kinases (Duchatelle-Gourdon et al. 1989; Horn and Korn 1992; Becq 1996; Tang and Hoshi 1999). In our experiments, the bath solution always contained ATP, either Na_2ATP or MgATP. However, ATP in the range of 2 to 5 mM failed to prevent single-channel current rundown. We also tested the effect of the catalytic subunit of protein kinase A (c-PKA) and alkaline phosphatase in the presence of MgATP. The addition of these agents involved in phosphorylation/dephosphorylation processes did not seem to modify the time course of rundown (data not shown).

Finally, the time course of the rundown did not present greater changes when the single-channel recordings were

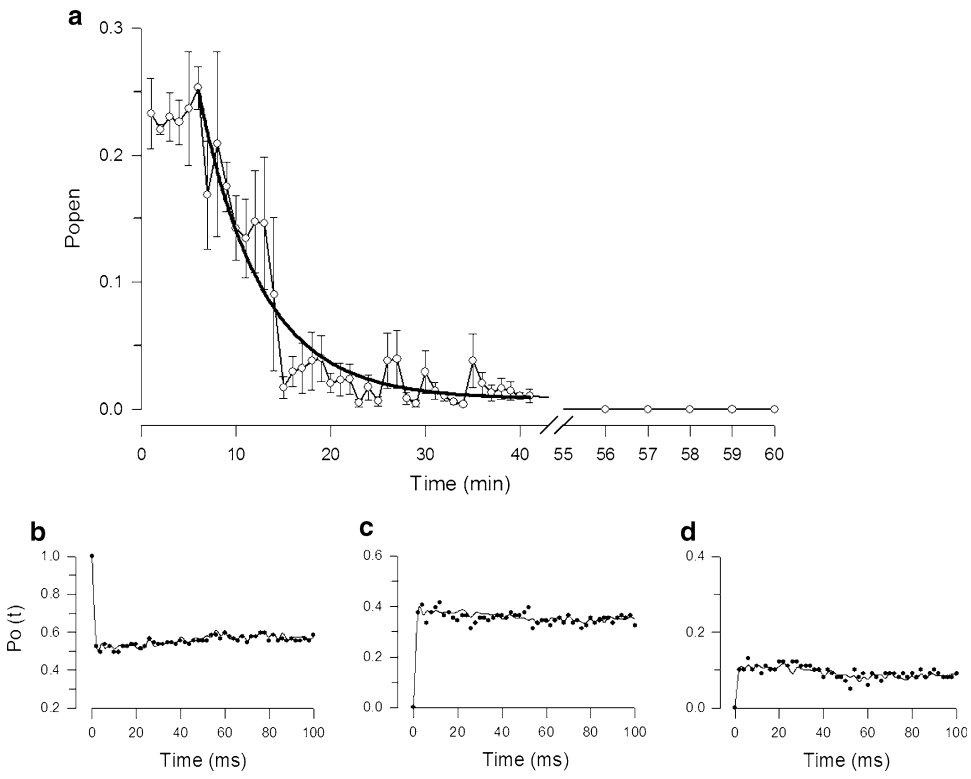

Fig. 2 Open probability as a function of time. **a** Rundown of the 16-pS K^+ channel. Time dependence of P_o at consecutive 100-ms sweeps at +40 mV. Inside-out recordings were started at time 0. The smooth line is a single-exponential fit, with a time constant of 5.7 min. Each point represents the mean ± SEM of P_o for 1 min. **b**, **c**, **d** Binomial analysis of the experiment depicted in Fig. 1. This patch contained two active channels. The points represent the probability of exactly zero (**b**), one (**c**), and two (**d**) channels as a function of time. The smooth line was fitted with the binomial theorem as described under results

performed in vesicle-attached configuration (data not shown). This suggests clearly that the vesicles were free of cytoplasmic components, as reported previously (Standen et al. 1985).

The following analysis was performed to examine the possibility that the channels behave independently of one another. The independent behavior of distinct populations of voltage-activated ion channels has been reported previously (Horn et al. 1984; Standen et al. 1985; Vázquez 1998). All our single-channel patch recordings had, at least, two active channels. A binomial analysis was performed to determine whether the 16-pS K^+ channel belongs to a homogeneous and independent population. Figure 2b–d depict three representative traces in which the number of simultaneously open channels is two. Considering that the channels have an independent behavior, the probability P_x of observing x channels open out of a total number N is represented by the binomial theorem:

$$P_x(t) = \binom{N}{r} \cdot P(t)^x \cdot [1 - P(t)]^{(N-x)} \quad (2)$$

where $P(t)$ is the probability of each channel being open at a given time. The points in Fig. 2 show the calculated probability of having exactly zero (Fig. 2b), one (Fig. 2c), and two (Fig. 2d) open channels, respectively, and the solid line represents the comparison with the theoretical prediction. There is a great agreement between the experimental result and the theoretical prediction, which suggests that the channels behave independently of one another and comprise a homogeneous population (Horn et al. 1984; Standen et al. 1985; Spruce et al. 1987; Hoshi and Aldrich 1988; Vázquez 1998).

Slow inactivation was evidenced by clusters of records without single-channel activity (blank records) during repetitive stimulation. The channels underwent this slow process when depolarizing pulses were applied at constant intervals of 1 s. Runs analysis was used to confirm that the slow inactivation does not occur randomly (Swed and Eisenhart 1943; Horn et al. 1984; Sigworth and Zhou 1992). This analysis of the data gave a Z-value of 6.4. This Z-value indicates that the blank records occurred in a non-random way. The slow inactivation induced the channels to be unable to open during seconds. A similar process has been described previously (Horn et al. 1984; Hoshi and Aldrich 1988; Martínez-Padrón and Ferrús 1997; Vázquez 1998). Slow inactivation was not observed in experiments with an interpulse interval >5 s ($n = 4$) (data not shown).

An estimation of the open probability (P_o) during voltage steps ranging from −40 to +40 mV showed that the gating of the 16-pS K^+ channel is voltage dependent. P_o was calculated by adding the total time the channel spent in the open state divided by the total time of the record of a given membrane potential. This method of estimation does not depend on how channels enter and leave open and closed states (Fenwick et al. 1982; Spruce et al. 1987). Thus, when P_o was determined, we found that it exhibits an apparent sigmoidal relationship with the patch membrane voltage (Table 1 and Fig. 4, open symbols).

Open time distributions could be fitted by the sum of two exponentials (data not shown). Time constants, fast and slow components, estimated from this fit are 0.19 ± 0.02 and 2.33 ± 0.036 ms at −40 mV and 0.28 ± 0.04 and 6.67 ± 0.01 ms at +40 mV ($n = 10$), respectively. The time constants increased with depolarization; this increase was slightly greater for the slower than for the fast component. The simplest gating mechanism that could account for the open time distribution of the 16-pS K^+ channel is a model with two open states. However, the corresponding states would be the product of more than one channel active in the patches (Colquhoun and Hawkes 1995). Moreover, since the channels are identical and are independent of one another, we can use the algorithm proposed by Fenwick et al. (1982) to obtain the mean open time (τ_o) for the 16-pS K^+ channel. From this algorithm, the τ_o should be

$$\tau_o = \frac{\sum jt_j}{n_c} \quad (3)$$

where jt_j is the total time that all channels are open, and n_c is the total number of closing. Based on the average values, τ_o increases with depolarization (Table 1), and this result is consistent with the values found by fitting the open-time histograms.

The 13-pS K^+ Channel

A separate population of channels could be identified by their activation near −60 mV and their chord conductance of 19.33 ± 0.23, 17.1 ± 1, and 12.90 ± 1.30 pS at −60, 0, and +40 mV, respectively ($n = 10$). This channel was classified as the 13-pS K^+ channel, according to its conductance at +40 mV. In 43 patches of 150, the depolarization steps evoked this kind of current.

Table 1 Open probability (P_o) and open time (τ_o) for the 16-pS K^+ channel: voltage dependence of open probability and open time (mean ± SEM)

Membrane potential (mV)	P_o	τ_o (ms)	N
−40	0.11 ± 0.01	1.03 ± 0.12	10
−20	0.16 ± 0.09	1.07 ± 0.14	10
0	0.26 ± 0.07	2.11 ± 0.08	10
+20	0.48 ± 0.11	3.56 ± 0.10	10
+40	0.57 ± 0.13	4.68 ± 0.11	10

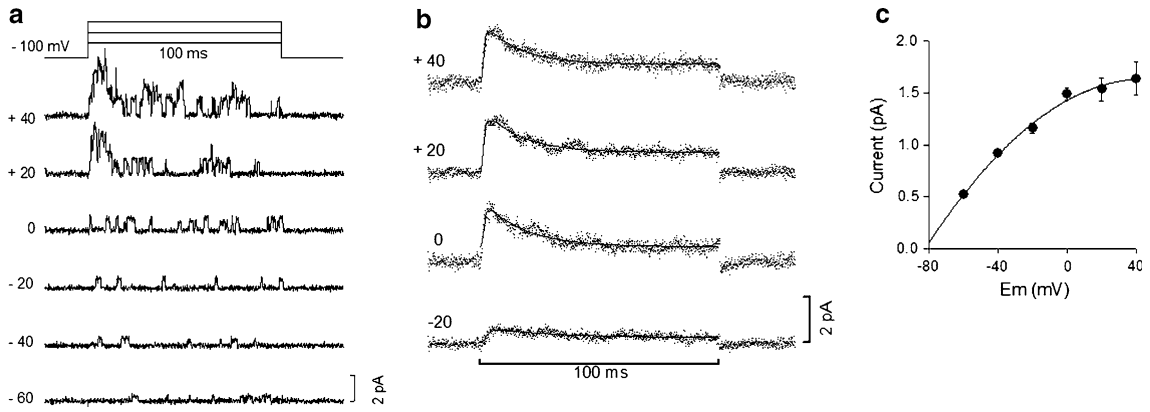

Fig. 3 Single-channel currents through the 13-pS K^+ channel. **a** Examples of outward unitary currents. Channels were active during voltage steps from a holding potential of −100 mV. **b** Ensemble average currents from a patch containing four channels. The number of sweeps averaged was 100 for all voltage steps. Smooth curves are best fits of the Hodgkin-Huxley kinetic model to data. **c** Mean single-channel current amplitude plotted against voltage step ($n = 10$); the curve was drawn visually through the experimental points. Data for a and b are from the same patch

Figure 3a shows single-channel currents at different membrane potentials. The mean current-voltage relationship from 10 experiments is illustrated in Fig. 3c. The current-voltage relationship was nonlinear, suggesting that the 13-pS K^+ channel rectified at depolarizing voltages, similarly to delayed rectifier currents (Standen et al. 1985). The extrapolated reversal potential was −88 ± 2.8 mV. The next step was to investigate the ionic selectivity. Thus, the K^+ ion in the pipette solution was increased to 120 mM; under this ionic condition, we found zero current around 0 mV (data not shown). From these results, it appears that the 13-pS K^+ channel is mainly permeable to the K^+ ion.

This single-channel K^+ channel gating behavior produces ensemble average currents that exhibited a fast activation along a sigmoid time course and then decayed partially and gradually from their maximum during voltage depolarization. These pseudomacroscopic K^+ currents were obtained from 100 individual recordings from a multichannel patch. Ensemble average currents reproduced qualitatively the main features of macroscopic K^+ currents in plasma membrane of skeletal muscle (Adrian et al. 1970; Stanfield 1970; Beam and Donaldson 1983; Hocherman and Bezanilla 1996). To obtain a quantitative comparison, we used the Hodgkin-Huxley (1952) kinetic model. The time course of the currents can be well described by Eq. 1 plus a single-exponential decay term (time constant of inactivation; τ_h) (Fig. 3b). However, at +40 mV, the decline in the current followed a more complex time course. Therefore, the sum of at least two exponential decay terms plus a steady-state term was needed. The activation time constant (τ_a) was voltage dependent, ranging from 1.69 ms at −20 to 0.60 ms at + 40 mV.

The gradual decline in the K^+ currents has been described as a relatively fast inactivation that ranges from a few milliseconds to several seconds (Adrian et al. 1970; Duval and Léoty 1980; Standen et al. 1985; Hoshi and Aldrich 1988; Rudy 1988; Zagotta et al. 1988; Jonas et al. 1989; Hocherman and Bezanilla 1996) (Fig. 3b). The time course of fast inactivation in the 13-pS channel varied considerably among the multichannel patches analyzed. At the membrane voltages shown in Fig. 3b, we found that the inactivation was independent of the voltage. The first time constant of inactivation is 29.6 ± 9.4 ms ($n = 5$), and at +40 mV the second time constant range is between 80 and 200 ms ($n = 10$).

Frequently, the 13-pS K^+ channels developed a process of slow inactivation during a series of pulses at 1-Hz stimulation. Indeed, blank sweeps are grouped. Runs analysis gave a Z-value of 3.86. This value of Z indicates that the observed clusters in time did not occur randomly. It has been suggested that slow inactivation would underlie fast inactivation (Adrian et al. 1970; Stanfield 1970; Standen et al. 1985). The role of slow inactivation in fast inactivation was investigated with an interpulse interval of 8 s, since we found that, at this stimulation frequency, the slow process of inactivation was apparently prevented (data not shown). Single-channel currents were recorded over a voltage range of −20 to 40 mV at a holding potential of −100 mV. Under these conditions, the time course of fast inactivation is apparently voltage independent, and again, varied considerably, following an exponential course, with the first τ_h ranging between 17.38 and 52.20 ms ($n = 5$). Again, the time course of fast inactivation at +40 mV is better described by a sum of at least two exponential terms; the fit of the second τ_h gave values of 87 to 244.74 ms ($n = 5$). There was great similitude in the time course of fast inactivation obtained from ensemble average currents when the interpulse interval was 1 s and when it was 8 s, suggesting that slow

inactivation is not involved in the gradual decay of average currents in this channel, although relatively fast inactivation might result from a decrease in the open probability during voltage step. Furthermore, simultaneous openings were seen almost immediately after depolarization, and then they decreased with time (Fig. 3a). In these multichannel patches, binomial analysis showed that the 13-pS K^+ channels have an independent gating behavior and belong to the same population (data not shown).

It is clear from the results described above that activation of the 13-pS K^+ channel is voltage dependent. However, in an attempt to characterize further the voltage dependence of the channel's kinetics, we analyzed the open probability (P_o) and the latency to the first opening as a function of the voltage membrane (Fig. 4). P_o was calculated from single-channel currents elicited by pulses at 20-mV intervals from −60 to +40 mV. Figure 4a (filled symbols) shows the P_o plotted against the voltage membrane. Data points are means and standard error computed from the same 10 experiments as shown in Fig. 3c. At these voltages, the P_o increases in an almost-linear fashion (Fig. 4a). Figure 4b, c depict the analysis of the latency to the first opening. The cumulative first latency histogram (Fig. 4b) shows that, at depolarizing potentials, the channels in closed state go faster to the first opening than they do at hyperpolarizing potentials. The mean first latencies are 12.57 ± 1.10 ms at −40 mV and 1.43 ± 0.13 ms at +40 mV (Fig. 4b). The latency to the first opening changed about ninefold over the potentials explored. The first latency results of the 13-pS K^+ channel indicate that the transitions before the first opening are voltage dependent, whereas the P_o results show their voltage dependence after the first opening. Figure 4c illustrates a typical histogram of the latency to the first opening at +40 mV, in which a delay and a peak greater than time 0 can be observed. The delay and the peak decreased with depolarization; this is consistent with our previous results. There is evidence that the voltage-gated channels do not open instantly upon depolarization, but rather must travel between few closed states before being opened for the first time (Patlak and Horn 1982; French and Horn 1983; Standen et al. 1985; Shao and Papazian 1993). To this point, the first-latency distributions, measured at 0, +20, and +40 mV, could be fitted by a model of three states (Patlak and Horn 1982; Standen et al. 1985; Vázquez 1998). The fitted curve for the first-latency distribution at +40 mV was exponential in form and had an initial peak, as shown in Fig. 4c. In this model, the fitting of two exponential components reflects a series of transitions between two closed states before the first opening. However, the peak of the fitted curve precedes that of the experimental data, suggesting the presence of more than two closed states (Fig. 4c).

The 7-pS K^+ Channel

We distinguished another single K^+-current channel as depicted in Fig. 5. This channel was characterized by its conductance of 7 pS at +40 mV. For that reason, we designated it the 7-pS K^+ channel. In response to depolarizing pulses ≥0 mV, the channel activated with a lengthened delay and a very low open probability (0.14 ± 0.02 at +40 mV). The K^+ channel was detected in 13 of 150 sarcolemma vesicles. Figure 5a shows 30 representative recordings of single-channel activity obtained during a single step at +40 mV from a −100 mV holding potential. Under the ionic conditions used, γ was 8.11 ± 0.320 and 6.90 ± 0.178 pS ($n = 10$) at 0 and at +40 mV, respectively. Ensemble average currents typically exhibited a great delay in their time course of activation (Fig. 5b). The runs analysis showed that this

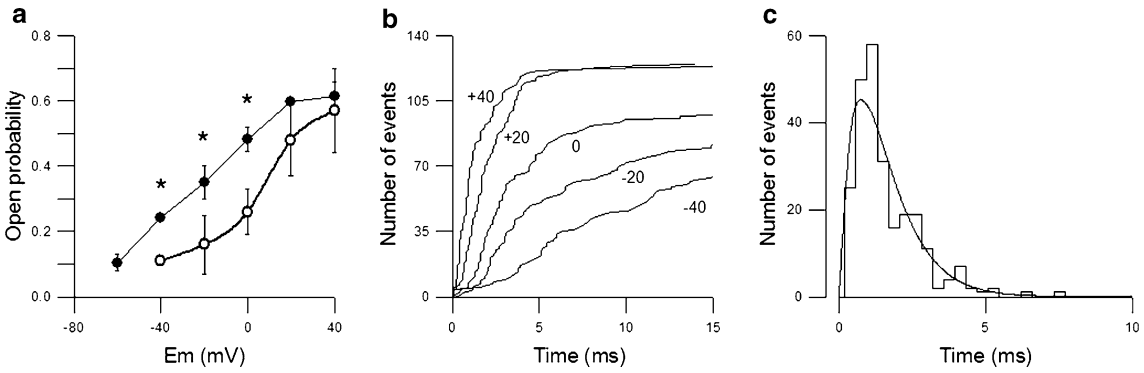

Fig. 4 Voltage dependence of the 13-pS K^+ channel. **a** Mean open probability in 10 different patches versus the voltage pulses. Filled symbols are mean values of 13-pS K^+ channels, and open symbols are mean values of 16-pS K^+ channels. Asterisks indicate significant differences ($p < 0.5$) as calculated using a paired t-test. **b** Cumulative latency-to-first-opening histograms. Mean first latencies were 12.57, 7.81, 3.83, 2.27, and 1.43 at −40, −20, 0, +20, and +40 mV, respectively. **c** Histogram of distribution of latencies to first opening at +40 mV. The smooth curve is the best fit of a three-state model to the data: $(f(t) = \frac{R_1 R_2}{R_1 - R_2}[exp(-R_2 t) - exp(-R_1 t)])$. All data are from the patches illustrated in Fig. 3

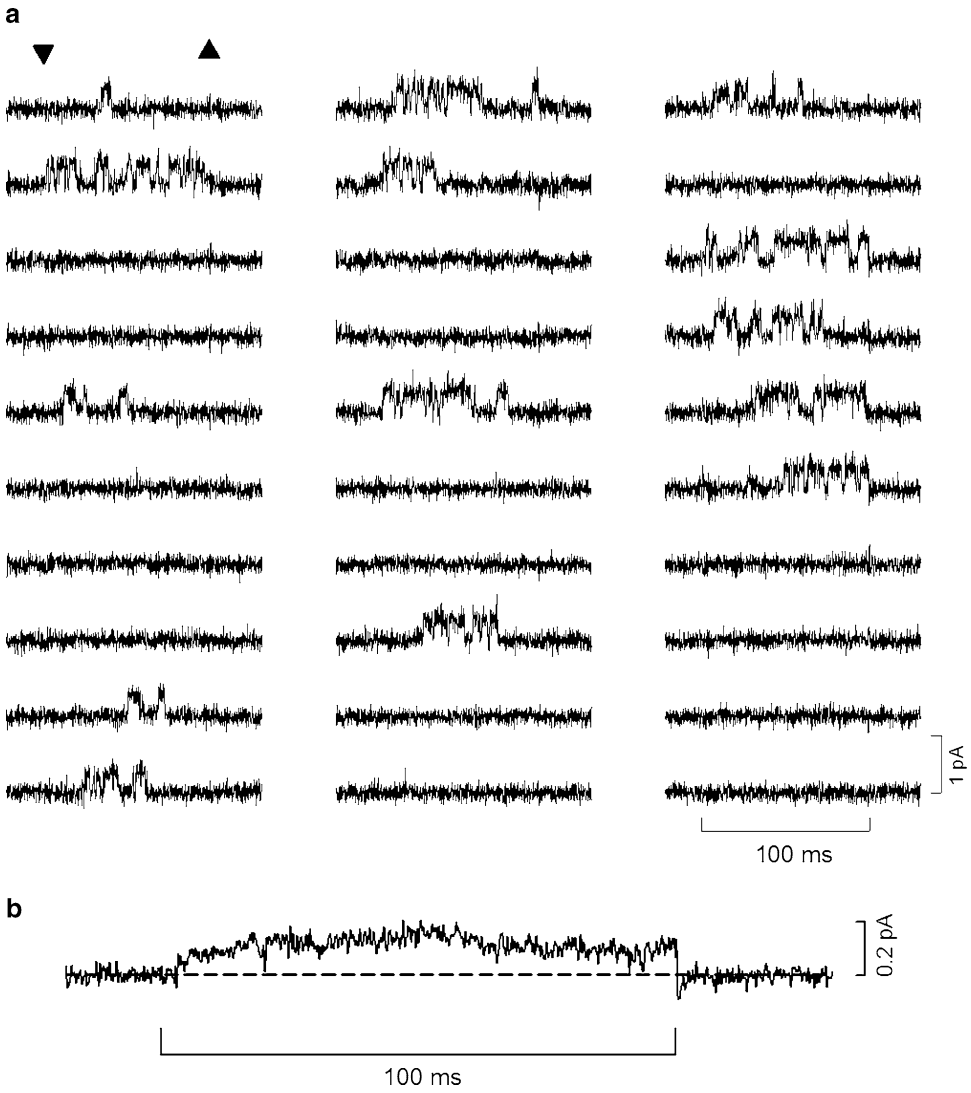

Fig. 5 Single-channel activity of the 7-pS K^+ channel. **a** Consecutive current records from a holding potential of −100 mV to +40 mV; 100-ms voltage steps indicated by arrowheads. Note that both blank and opening-channel records show the clustering pattern. The interpulse interval was 1 s. **b** Ensemble average current is the average of 100 individual sweeps

channel developed nonrandom clusters similar to the slow inactivation process.

In contrast to all inside-out patches analyzed previously, each of which contained a single class channel, we obtained 10 patches containing two of the three different types of K^+ channels described herein. Although it was uncommon to observe all three types of K^+ channels in a single patch, at least the 16- and 13-pS K^+ channels were often recorded in the same patch (Fig. 6a). Figure 6a shows representative unitary currents at +40 mV from a −100-mV holding potential. We did not observe any significant differences in their conductance when they were observed alone versus when they were recorded simultaneously. When the ensemble average currents were reached, the time course of activation rose along a sigmoid curve until a maximum, and subsequently, the current declined almost to a steady state (Fig. 6b), in a very similar way as it does in skeletal muscle fiber (Adrian et al. 1970; Stanfield 1970; Beam and Donaldson 1983; Hocherman and Bezanilla 1996). The smooth curve (larger trace in Fig. 6b) was calculated by an equation similar to Eq. 1, but in order to obtain the best fit, we used the equation plus an exponential decay term and a constant term. In the same experiment and 12 min after the excision, the peak of the ensemble average current decreased to about 34% of the peak of the ensemble obtained immediately after excision (smaller trace in Fig. 6b). Likewise, at the end of the pseudomacroscopic current, there was a reduction of about 50%. This decrease in the amplitude of the average current could indicate the presence of the rundown process of the 16-pS K^+ channel.

The sensitivity of the three voltage-activated K^+ channels to external application of tetraethylammonium chloride (TEA-Cl) was examined. We applied 5 mM TEA-Cl instead of 5 mM NaCl to the external membrane surface by adding it to the pipette solution. In the excised patches ($n = 15$), the addition of TEA-Cl blocked the unitary currents. The block of the single-channel K^+ currents did

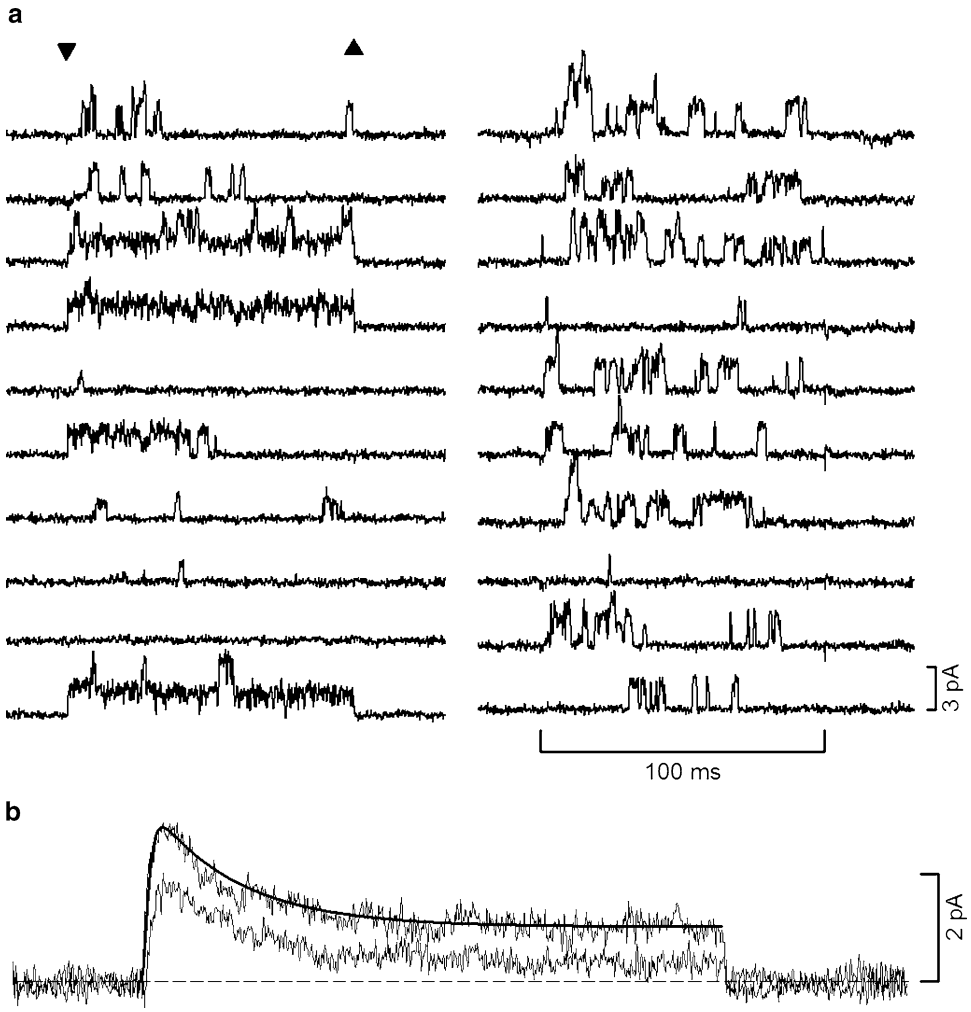

Fig. 6 Recording of the 16- and 13-pS K^+ channels in the same patch. **a** Twenty consecutive single-channel records are shown from a holding potential of −100 mV to +40 mV of voltage step. Current traces were recorded immediately after seal formation, i.e., at 0 min. Current traces on 3rd, 4th, 6th, and 10th records depict the 16-pS K^+ channel, which typically showed long duration openings interrupted by brief closings, similar to those in Fig. 1. The second type of single-channel activity, which is prominent in the 11th through the 20th records, corresponds to the 13-pS K^+ channel, similar to those in Fig. 3. **b** Comparison of the ensemble average currents at 0 min (higher average current) and 14 min later (lower average current). The smooth curve is the best fit of the data to a modified Hodgkin-Huxley model (details are given in the text). All data are from the same patch

not seem to be affected by further changes in TEA-Cl concentrations, we never saw any unitary activity when 2 mM TEA-Cl was in the pipette solution ($n = 10$). Therefore, the simplest assumption of the effect of TEA was a total block of all three K^+ channels. On the other hand, the addition of 5 mM 4-AP to the pipette solutions did not block any of the three distinct K^+ channels (Adams et al. 1980; Zagotta et al. 1988; Hille 1992; Weiss et al. 2001; Liu et al. 2008). However, it has been reported that the delayed rectifier is blocked by intracellular application of 4-AP (Gu et al. 2001; Tammaro et al. 2004). Therefore, experiments were conducted to investigate the intracellular effects of 4-AP on the three voltage-dependent K^+ channels. In four more experiments, internal application of 4-AP did not affect the single-channel currents, just like its external effects (data not shown).

Discussion

The main finding of this study is that there are three types of voltage-gated K^+ currents in membrane vesicles from frog skeletal muscle. All three types of K^+ currents were characterized in the inside-out patch-clamp configuration, under the same ionic conditions and same voltage protocols. We observed that the channels active at a depolarizing membrane potential displayed the same conductance for both the cell-attached and the inside-out patch-clamp configurations. The single-channel K^+ currents are readily distinguishable based on the voltage at which they activate, their open probability, and their single-channel conductance. The extrapolated reversal potential for these K^+ currents, estimated from current-voltage relationships, indicates that the channels are mainly permeable to K^+ (Figs. 1 and 3). In addition, the Hodgkin-Huxley (1952) kinetic model provides a fair description of the ensemble average currents of the 16- and 13-pS K^+ channels; therefore, we categorized them as members of the delayed rectifier family (Rudy 1988). Further, our single-channel currents were blocked by TEA, a K^+-channel blocker that has proved helpful in identifying delayed rectifier K^+ channels (Hille 1992). Taken together, these observations suggest that these three voltage-activated K^+ channels can be classified as delayed rectifiers.

Delayed rectifier K^+ channels in several different preparations have been characterized as sensitive and insensitive to 4-AP (Adams et al. 1980; Zagotta et al. 1988; Hille 1992; Coetzee et al. 1999; Gu et al. 2001; Weiss et al. 2001; Tammaro et al. 2004; Liu et al. 2008). Although the potassium current blocker, 4-AP, is membrane permeable and can act on K^+ channels, either inside or outside; in this study, none of the K^+ currents were blocked by intracellular or extracellular 4-AP, as previously reported (Adams et al. 1980; Zagotta et al. 1988; Hille 1992; Weiss et al. 2001; Liu et al. 2008).

The delayed rectifier K^+ currents that produce a sustained or a declined outward current have been measured in several cell types (Hodgkin and Huxley 1952; Hille 1967; Adrian et al. 1970; Stanfield 1970; Beam and Donaldson 1983; Bezanilla et al. 1986; Llano et al. 1988; Bernheim et al. 1996; Yeoman and Benjamin 1999; Chen and Johnston 2004). As already discussed, the time course of K^+ currents can be described by the Hodgkin-Huxley (1952) equations. Thus, the time course of the 16-pS K^+ channel activation was quantified by fitting the ensemble average currents to n^4 kinetics (Eq. 1). On the basis of this analysis, we can conclude that this type of K^+ channel produced voltage-dependent and noninactivating K^+ currents (Fig. 1), similarly to the macroscopic and single-channel currents recorded in squid giant axon (Hodgkin and Huxley 1952; Llano et al. 1988), in myelinated nerve fibers (Hille 1967; Dubois 1981), and in muscle cells (Trautmann et al. 1986; Jospin et al. 2002). On the other hand, our recordings revealed an additional 13-pS K^+ channel. Because this outward currents decay relatively rapidly, we fitted n^4 h to the data obtained from ensemble average currents (Fig. 3). The decaying current reported here shows that the 13-pS delayed rectifier K^+ channel displays inactivation, which has also been observed in skeletal muscle (Adrian et al. 1970; Stanfield 1970; Duval and Léoty 1980; Pappone 1980; Beam and Donaldson 1983; Standen et al. 1984; Trautmann et al. 1986; Rudy 1988; Brinkmeier et al. 1991; Hocherman and Bezanilla 1996) and in neurons (Bouskila and Dudek 1995). The third K^+ current, the 7-pS K^+ channel, appears with strong depolarization from a holding potential of −100 mV. The ensemble average currents of this channel are characterized by a great delay and very slow activation (Fig. 5). The channel gating is similar to that reported for the potassium channel in squid giant axon, even though important differences exist between their conductances (Llano et al. 1988).

The three types of unitary K^+ channel currents are readily distinguishable by their different unitary conductance in asymmetrical KCl ionic conditions. Single-channel conductance of the 16-pS K^+ channel is well matched to single-channel conductance of the delayed rectifier K^+ channel recorded in squid giant axon (Llano et al. 1988; Perozo et al. 1991), in skeletal muscle (Hocherman and Bezanilla 1996), in neurons (Chen and Johnston 2004), and in expressed Kv1.2 and Kv3.1a channels (Shahidullah et al. 1995). The single-channel conductance of the 13-pS K^+ channel is comparable to the unitary conductance for the delayed rectifier channels present in cultured microglia (Schilling et al. 2000), in skeletal muscle (Standen et al. 1985; Brinkmeier et al. 1991), in expressed Kv1.2 and Kv3.1a channels (Shahidullah et al. 1995), and in cultured neurons (Rogawski 1986). Finally, the third type of K^+ channel has a single-channel conductance of 7 pS. This conductance matches those of the delayed rectifiers recorded from expressed human delayed rectifier (h-DRK1) (Benndorf et al. 1994), myelinated nerve fibers (Jonas et al. 1989; Koh and Vogel 1996), expressed vascular smooth muscle Kv1.5 (Clément-Chomienne et al. 1999), vascular smooth cells (Karle et al. 1998), and human myoblasts (Bernheim et al. 1996).

Our results show that single-channel activities could be observed only after the channel had been activated at depolarizing voltages (Figs. 1, 3, and 4 and Table 1). In addition, upon depolarization, all three types of K^+ channels became activated at different voltage ranges, and their open channel durations and open probabilities increased with voltage (Fig. 4 and Table 1). Therefore, we concluded that the gating current behavior of the three potassium channels is voltage dependent. This is in agreement with single-channel measurements of delayed rectifiers reported for skeletal muscle (Standen et al. 1985; Hocherman and Bezanilla 1996), squid axons (Conti and Neher 1980; Llano et al. 1988), synaptic buttons (Martínez-Padrón and Ferrús 1997), and neurons (Chen and Johnston 2004).

Single-channel currents due to the 16-pS K^+ channel exhibited rundown in either recording condition, vesicle-attached and inside-out. Rundown shows properties similar to those described for delayed rectifier, NMDA, calcium, and ATP-dependent K^+ channels (Shao and Papazian 1993; McKillen et al. 1994; Becq 1996; Hocherman and Bezanilla 1996; Jospin et al. 2002). Our results are in good agreement with a previous report (Hocherman and Bezanilla 1996) concerning the effects of phosphorylating agents on the rundown process. That is, neither ATP (Na^+ and Mg^{2+}), nor c-PKA, nor alkaline phosphatase has proven helpful in preventing or reverting the rundown of 16-pS K^+ single-channel currents. We did not perform systematic experiments designed to identify the mechanisms underlying this process. However, it appears that cytoskeletal interaction may be involved in the rundown process, as has been reported previously (Rosenmund and Westbrook 1993; Nörenberg et al. 1999). Certainly, more experiments are required to determine the mechanism of the rundown process.

Based on our runs analysis, we found that all three voltage-gated K^+ channels exhibited a process called slow inactivation, characterized by a nonrandom gating behavior pattern. This slow inactivation is comparable to that previously described in the literature (Horn et al. 1984; Standen et al. 1985; Martínez-Padrón and Ferrús 1997; Vázquez 1998). We also observed that the channels did not exhibit slow inactivation (data not shown) at intervals longer than the time necessary for the channels to go into and out of the slow process (Horn et al. 1984). However, ensemble average currents of the 13-pS K^+ channel displayed the N-type inactivation when the slow inactivation process was prevented. Although we did not systematically explore the mechanism underlying the distinct inactivation processes, it might be concluded that the fast and slow inactivation processes of the 13-pS K^+ channel occur in an independent manner. On the other hand, the fact of preventing slow inactivation is not critical for the loss of activity of the 16-pS K^+ channel by the rundown process.

In summary, this study reveals that in vesicles from the sarcolemma of frog skeletal muscle there are three distinguishable types of single-channel K^+ currents. The biophysical and pharmacological properties led us to conclude that the three single-channel currents consist primarily of delayed rectifier K^+ currents (Adrian et al. 1970; Stanfield 1970; Standen et al. 1985; Llano et al. 1988; Rudy 1988; Hille 1992; Hocherman and Bezanilla 1996). Indeed, delayed rectifier K^+ channels are important in controlling the rate of repolarization of the action potential in the membrane surface of skeletal muscle (Rudy 1988; Hille 1992). Because the 16- and 13-pS K^+ channels were found more frequently and the time course of their ensemble average currents resembles very closely those of macroscopic delayed rectifier K^+ currents (Adrian et al. 1970; Beam and Donaldson 1983; Hocherman and Bezanilla 1996), we assume that these two channels are the main contributors to the delayed rectifier K^+ currents in the sarcolemma of frog skeletal muscle. In a previous paper, we described the single-channel properties of A-type K^+ channel in the frog skeletal muscle (Vázquez 1998). Here we obtained evidence that delayed-rectifier outward K^+ currents are composed of three components. It is well known that voltage-gated K^+ channels underlie firing patterns in excitable cells (Hille 1992). Therefore, attention should be given to understanding the role of each one of them in the cellular excitability of skeletal muscle. Finally, the present findings open the way for new experimental approaches that would allow confirmation of this diversity of voltage-gated K^+ channels in skeletal muscle cell membrane.

Acknowledgments We thank Dr. David E García for critical reading of the manuscript, as well as Mr. Amado García and Mr. Roberto Reyes for their excellent technical assistance.

References

Adrian RH, Chandler WK, Hodgkin AL (1970) Slow changes in potassium permeability in skeletal muscle. J Physiol (Lond) 208:645–668

Adams DJ, Smith SJ, Thompson SH (1980) Ionic currents in molluscan soma. Annu Rev Neurosci 3:141–167

Barrett JN, Magleby KL, Pallotta BS (1982) Properties of single calcium-activated potassium channels in cultured rat muscle. J Physiol (Lond) 331:211–230

Beam KG, Donaldson PL (1983) A quantitative study of potassium channel kinetics in rat skeletal muscle from 1 to 37°C. J Gen Physiol 81:485–512

Becq F (1996) Ionic channel rundown in excised membrane patches. Biochim Biophys Acta 1286:53–63

Benndorf K, Koopmann R, Lorra C, Pongs O (1994) Gating and conductance properties of a human delayed rectifier K+ channel expressed in frog oocytes. J Physiol (Lond) 477:1–14

Bernheim L, Liu JH, Hamann M, Haenggeli CA, Fischer-Lougheed J, Bader CR (1996) Contribution of a non-inactivating potassium current to the resting membrane potential of fusion-competent human myoblasts. J Physiol (Lond) 493:129–141

Bezanilla F, Caputo C, DiPolo R, Rojas H (1986) Potassium conductance of the squid giant axon is modulated by ATP. Proc Natl Acad Sci USA 83:2743–2745

Brinkmeier H, Zachar E, Rüdel R (1991) Voltage-dependent K+ channels in the sarcolemma of mouse skeletal muscle. Pflügers Arch 419:486–491

Bouskila Y, Dudek FE (1995) A rapidly activating type of outward rectifier K+ current and A-current in rat suprachiasmatic nucleus neurones. J Physiol (Lond) 488:339–350

Chen X, Johnston D (2004) Properties of single voltage-dependent K+ channels in dendrites of CA1 pyramidal neurones of rat hippocampus. J Physiol (Lond) 559:187–203

Clément-Chomienne O, Ishii K, Walsh MP, Cole WC (1999) Identification, cloning and expression of rabbit vascular smooth muscle Kv15 and comparison with native delayed rectifier K+ current. J Physiol (Lond) 515:653–667

Coetzee WA, Amarillo Y, Chiu J, Chow A, Lau D, McCormack T, Moreno H, Nadal MS, Ozaita A, Pountney D, Saganich M, Vega-Saenz de Miera E, Rudy B (1999) Molecular diversity of K+ channels. Ann NY Acad Sci 868:233–285

Colquhoun D, Hawkes AG (1995) The principles of the stochastic interpretation of ion-channel mechanisms. In: Sakmann B, Neher E (eds) Single-channel recording, 2nd edn. Plenum, New York, pp 397–482

Colquhoun D, Sigworth FJ (1995) Fitting and statistical analysis of single-channel records. In: Sakmann B, Neher E (eds) Single-channel recording, 2nd edn. Plenum, New York, pp 483–585

Conti F, Neher E (1980) Single channel recordings of K+ currents in squid axons. Nature 285:140–143

Dubois JM (1981) Evidence for the existence of three types of potassium channels in the frog Ranvier node membrane. J Physiol (Lond) 318:297–316

Duchatelle-Gourdon I, Hartzell HC, Lagrutta AA (1989) Modulation of the delayed rectifier potassium current in frog cardiomyocytes by beta-adrenergic agonists and magnesium. J Physiol (Lond) 415:251–274

Duval A, Léoty C (1980) Comparison between the delayed outward current in slow and fast twitch skeletal muscle in the rat. J Physiol (Lond) 307:43–57

Fenwick EM, Marty A, Neher E (1982) A patch-clamp study of bovine chromaffin cells and of their sensitivity to acetylcholine. J Physiol (Lond) 331:577–597

French RJ, Horn R (1983) Sodium channel gating: models, mimics, and modifiers. Annu Rev Biophys Bioeng 12:319–356

Gu Y, Preston MR, El Haj AJ, Howl JD, Publicover SJ (2001) Three types of K(+) currents in murine osteocyte-like cells (MLO-Y4). Bone 28:29–37

Hamill OP, Marty A, Neher E, Sakmann B, Sigworth FJ (1981) Improved patch-clamp techniques for high-resolution current recording from cells and cell-free membrane patches. Pflügers Arch 391:85–100

Hille B (1967) The selective inhibition of delayed potassium currents in nerve by tetraethylammonium ion. J Gen Physiol 50:1287–1302

Hille B (1992) Ionic channels of excitable membranes, 2nd edn. Sinauer Associates, Sunderland, MA

Hocherman SD, Bezanilla F (1996) A patch-clamp study of delayed rectifier currents in skeletal muscle of control and mdx mice. J Physiol (Lond) 493:113–128

Hodgkin AL, Huxley AF (1952) A quantitative description of membrane current and its application to conduction and excitation in nerve. J Physiol 117:500–544

Horn R, Korn SJ (1992) Prevention of rundown in electrophysiological recording. Methods Enzymol 207:149–155

Horn R, Vandenberg CA, Lange K (1984) Statistical analysis of single sodium channels. Effects of N-bromoacetamide. Biophys J 45:323–335

Hoshi T, Aldrich RW (1988) Gating kinetics of four classes of voltage-dependent K+ channels in pheochromocytoma cells. J Gen Physiol (Lond) 91:107–131

Jonas P, Bräu ME, Hermsteiner M, Vogel W (1989) Single-channel recording in myelinated nerve fibers reveals one type of Na channel but different K channels. Proc Natl Acad Sci USA 86:7238–7242

Jospin M, Mariol MC, Ségalat L, Allard B (2002) Characterization of K (+) currents using an in situ patch clamp technique in body wall muscle cells from Caenorhabditis elegans. J Physiol (Lond) 544:373–384

Karle CA, Yao X, Kreye VA (1998) A K^+ single channel and whole-cell clamp study on the effects of levocromakalim in guinea pig portal vein cells. Naunyn Schmiedebergs Arch Pharmacol 358:374–381

Koh DS, Vogel W (1996) Single-channel analysis of a delayed rectifier K+ channel in Xenopus myelinated nerve. J Membr Biol 149:221–232

Liu YR, Ye WL, Zeng XM, Ren WH, Zhang YQ, Mei YA (2008) K+ channels and the cAMP-PKA pathway modulate TGF-beta1-induced migration of rat vascular myofibroblasts. J Cell Physiol 216:835–843

Llano I, Webb CK, Bezanilla F (1988) Potassium conductance of the squid giant axon. Single-channel studies. J Gen Physiol (Lond) 92:179–196

Martínez-Padrón M, Ferrús A (1997) Presynaptic recordings from Drosophila: correlation of macroscopic and single-channel K+ currents. J Neurosci 17:3412–3424

Marty A (1989) The physiological role of calcium-dependent channels. Trends Neurosci 12:420–424

McKillen HC, Davies NW, Stanfield PR, Standen NB (1994) The effect of intracellular anions on ATP-dependent potassium channels of rat skeletal muscle. J Physiol (Lond) 479:341–351

Nörenberg W, Hofmann F, Illes P, Aktories K, Meyer DK (1999) Rundown of somatodendritic *N*-methyl-D-aspartate (NMDA) receptor channels in rat hippocampal neurones: evidence for a role of the small GTPase RhoA. Br J Pharmacol 127:1060–1063

Pappone PA (1980) Voltage-clamp experiments in normal and denervated mammalian skeletal muscle fibres. J Physiol (Lond) 306:377–410

Patlak J, Horn R (1982) Effect of N-bromoacetamide on single sodium channel currents in excised membrane patches. J Gen Physiol 79:333–351

Perozo E, Jong DS, Bezanilla F (1991) Single channel studies of the phosphorylation of K+ channels in the squid giant axon. II. Nonstationary conditions. J Gen Physiol 98:19–34

Rogawski MA (1986) Single voltage-dependent potassium channels in cultured rat hippocampal neurons. J Neurophysiol 56:481–493

Rosenmund C, Westbrook GL (1993) Calcium-induced actin depolymerization reduces NMDA channel activity. Neuron 10:805–814

Rudy B (1988) Diversity and ubiquity of K channels. Neuroscience 25:729–749

Schilling T, Quandt FN, Cherny VV, Zhou W, Heinemann U, Decoursey TE, Eder C (2000) Upregulation of Kv13 K (+) channels in microglia deactivated by TGF-beta. Am J Physiol Cell Physiol 279:C1123–C1134

Shahidullah M, Hoshi N, Yokoyama S, Kawamura T, Higashida H (1995) Slow inactivation conserved in heteromultimeric voltage-dependent K+ channels between Shaker (Kv1) and Shaw (Kv3) subfamilies. FEBS Lett 371:307–310

Shao XM, Papazian DM (1993) S4 mutations alter the single-channel gating kinetics of Shaker K+ channels. Neuron 11:343–352

Sigworth FJ, Zhou J (1992) Ion channels. Analysis of nonstationary single-channel currents. Methods Enzymol 207:746–762

Spruce AE, Standen NB, Stanfield PR (1987) Studies of the unitary properties of adenosine–5′-triphosphate-regulated potassium channels of frog skeletal muscle. J Physiol (Lond) 382:213–236

Standen NB, Stanfield PR, Ward TA, Wilson SW (1984) A new preparation for recording single-channel currents from skeletal muscle. Proc R Soc Lond B Biol Sci 221:455–464

Standen NB, Stanfield PR, Ward TA (1985) Properties of single potassium channels in vesicles formed from the sarcolemma of frog skeletal muscle. J Physiol (Lond) 364:339–358

Stanfield PR (1970) The effect of the tetraethylammonium ion on the delayed currents of frog skeletal muscle. J Physiol (Lond) 209:209–229

Swed FS, Eisenhart C (1943) Tables for testing randomness of grouping in a sequence of alternatives. Annu Math Stat 14:66–87

Tammaro P, Smith AL, Hutchings SR, Smirnov SV (2004) Pharmacological evidence for a key role of voltage-gated K+ channels in the function of rat aortic smooth muscle cells. Br J Pharmacol 143:303–317

Tang XD, Hoshi T (1999) Rundown of the hyperpolarization-activated KAT1 channel involves slowing of the opening transitions regulated by phosphorylation. Biophys J 76:3089–3098

Trautmann A, Delaporte C, Marty A (1986) Voltage-dependent channels of human muscle cultures. Pflugers Arch 406:163–172

Vázquez M (1998) Single-channel analysis of fast transient outward K+ currents in frog skeletal muscle. Pflugers Arch 436:95–103

Weiss T, Erxleben C, Rathmayer W (2001) Voltage-clamp analysis of membrane currents and excitation-contraction coupling in a crustacean muscle. J Muscle Res Cell Motil 22:329–344

Yeoman MS, Benjamin PR (1999) Two types of voltage-gated K(+) currents in dissociated heart ventricular muscle cells of the snail Lymnaea stagnalis. J Neurophysiol 82:2415–2427

Zagotta WN, Brainard MS, Aldrich RW (1988) Single-channel analysis of four distinct classes of potassium channels in Drosophila muscle. J Neurosci 8:4765–4779